



Design and Integration of Planar Inductances on PCB Application Passive Type Filters

Nisrine Senhadji¹ · Azzedine Hamid² · Vincent Bley³ · Thierry Leby³

Received: 23 April 2019 / Revised: 27 November 2019 / Accepted: 31 December 2019 / Published online: 6 January 2020
© The Korean Institute of Electrical and Electronic Material Engineers 2020

Abstract

This paper is a synthesis of work encompassing simulation and experimental results aimed at designing, manufacturing and characterizing various fixed and variable width circular and square spiral inductance topologies deposited on a PCB-FR4 substrate. These inductors will compose filters for different applications of electronics and low power electronics. These prototypes of planar inductances were made at LAPLACE laboratory in Toulouse.

Keywords Planar inductor · Integration · Filter · PCB

1 Introduction

Power electronics is currently evolving towards integration, as a result of the constraints related to the need to miniaturize but also to reduce manufacturing costs. In many cases, hybrid systems offer volume reduction possibilities and the passive components, inductance, transformer and capacitor, represent a brake on this miniaturization. Inductive components such as coils or transformers are key elements of power electronics. These are well known and mastered components with regard to their discrete form, but their integration is still at the study stage and is still far from industrialization, [1–3]. In this work, we will focus on the design,

manufacture and characterization of spiral planar coils on PCB-FR4 [4] it is a composite used in electronic printed circuit boards. It is composed of an epoxy resin matrix and loaded with 8 folds of glass fibers woven in 0°/90° directions. The design of a PCB substrate inductor is difficult to modify once built on the PCB. The advantage of this technology who using lithographic techniques and microvia technology is now able to produce devices with micron precision and almost as small a size [5, 6]. We have targeted two types of coils: We have considered two types of inductors: standard and tapered inductors. The second type of inductor is characterised by an increasing track width according to the radius. This approach is of particular interest to the inductor as the total DC resistance will be effectively reduced to a given number of turns. Indeed, on one hand, this will compensate for the variation of the resistance linked to the increase of the conductor width of the inductor and on the other hand, it will reduce the proximity effect and the capacitive effect between turn. The gain is less perceptible because we have considered the same occupied space to all prototypes of inductors studied. This study has targeted the following topologies: circular, square which are represented in Fig. 1. The parameters that have been taken into account in this study are the topology, the turns' width, the interturn distance and the thickness of the conductor. The production and the characterization took place in the Laboratory on Plasma and Conversion of Energy UMR5213, Team MDCE, Toulouse, France [7].

✉ Nisrine Senhadji
senhadjinisrine@outlook.fr

Azzedine Hamid
hamidazdean@yahoo.fr

Vincent Bley
Vincent.bley@laplace.univ-tlse.fr

Thierry Leby
Thierry.lebey@laplace.univ-tlse.fr

¹ Departement of Electrotechnical, Faculty of Electrical Engineering, University of Sciences and Technology of Oran "Mohamed Boudiaf" (USTO), BP 1505, El Manouer, 31000 Oran, Algeria

² Nour Bachir University Center, El Bayadh, Algeria

³ LAPLACE Laboratory, University of Paul Sabatier, Toulouse, France

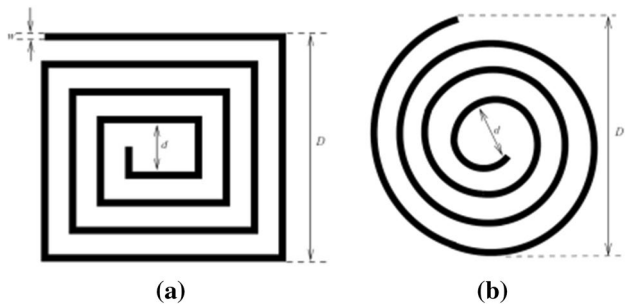


Fig. 1 Different forms of studied topologies [8]

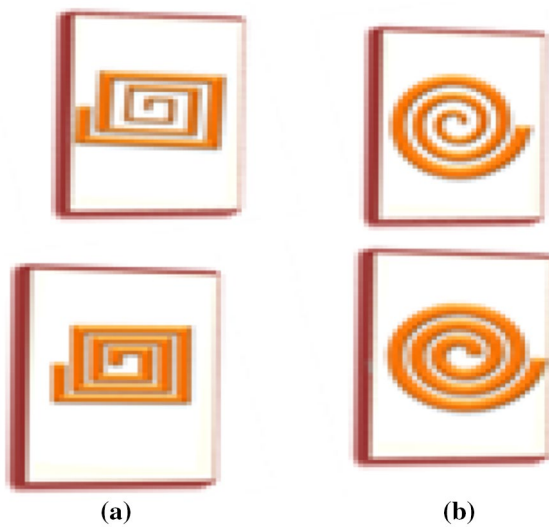


Fig. 2 Different prototypes of integrated coils realized a square, b circular

2 Experimental

2.1 Presentation of the Different Topologies of Planar Integrated Coils Studied

The studied topologies are presented in Fig. 1. These are the square and circular topologies.

2.2 Presentation of Realized Prototypes

Figure 2 presents the prototypes of planar integrated coils realized in this study.

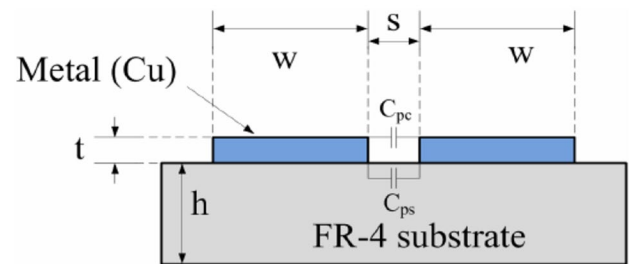


Fig. 3 Geometrical parameters of a square-shaped PCB inductor: view of the PCB inductor

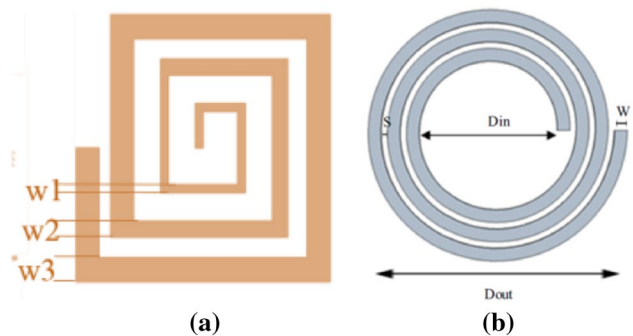


Fig. 4 Representation of different widths in inductance with variable width a and fixed width b

2.3 Planar Inductances' Characteristics

In this section, we present the geometrical and electrical characteristics of standard and tapered inductors [1, 9] (Fig. 3).

For a given form, an inductance is characterized, as shown in Fig. 4, by the number of turns n , the width of the conductor w , the spacing between turns s , the thickness t of conductor, the conductor's total length l_t , the average diameter, the diameters outside and inside d_{out} and d_{in} . The dimensions of the different topologies are as follows: $d_{out} = 10$ mm, $d_{in} = 1$ mm, $n = 3$ and $t = 35$ μm . For a three-turn variable-width coil, w_1 , w_2 and w_3 are the winding widths of each tower, as shown in Fig. 4.

2.4 Determination of Geometric Parameters

2.4.1 Calculation of the Length

The total length of the inductance is given by the following expression:

$$l_t = n d_{avg} N \tan\left(\frac{\pi}{N}\right) \quad (1)$$

For a square inductor, $N=4$. N is a big number for the circular inductor, where we get the expressions of the total length l_t , Eq. (2).

$$l_t = \frac{\pi}{2} [2nd_{in} + n(n+1)w + (n-1)ns] \tag{2}$$

$$\text{with } d_{avg} = \frac{d_{out} + d_{in}}{2} \tag{3}$$

2.4.2 Calculation of the Spacing Between Turns s

The following expression we have developed allows us to calculate the inter turns

$$s = \frac{d_{out} - d_{in} - 2nw}{(n+1)} \tag{4}$$

This expression is applicable for all cases. In the case of our coil: $n=3$ et $d_{in}=1$ mm et $d_{out}=10$ mm et $w=0.9$ mm, $s=0.54$ mm.

2.5 Integrated Planar Micro Inductance Manufacturing Process on PCB-FR4

The fabrication process concerns different integrated inductance topologies on a substrate of PCB-FR4 [1] for different thicknesses (0.3 mm, 0.9 mm, 1.6 mm). The copper conductor is deposited on the substrate. [10, 11]. These

prototypes were made at LAPLACE laboratory in Toulouse (LAPLACE) [7].

2.5.1 Cuttingsteps of PCB parts

We cut out 1.5×1.5 cm² PCB-FR4 substrate parts for different thicknesses 0.3, 0.9, 1.6 mm, by the chainsaw shown in Fig. 5. This substrate is a support of insulating material intended for receive the impression of an electrical or electronic circuit and the various components of this circuit to form hybrid or monolithic circuits. Copper windings of 35 μm thickness are then assembled on these substrates (PCB-FR4) (Figs. 6, 7, 8, 9, 10, 11, 12, 13 and 14).

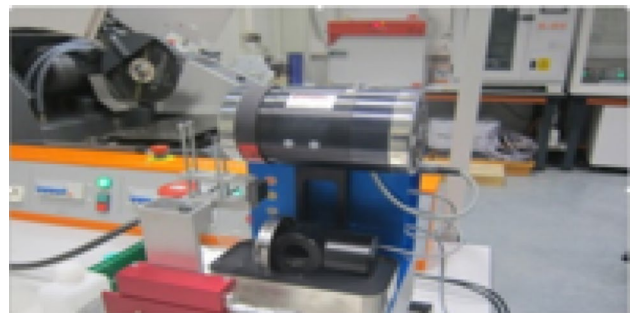


Fig. 6 Complete cutting equipment

Fig. 5 Manufacturing process [11]

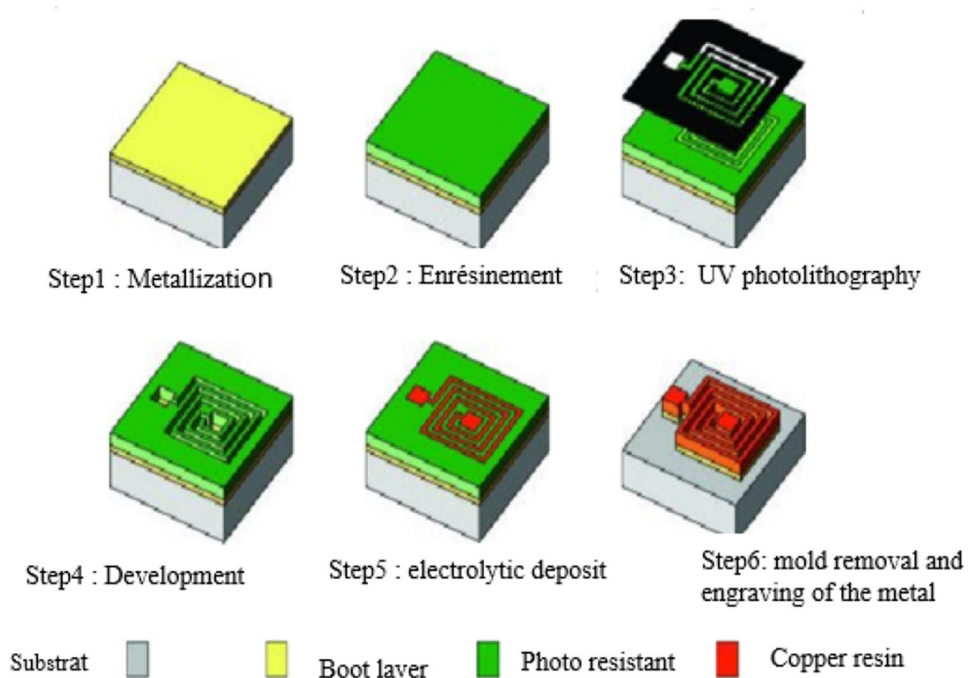




Fig. 7 Chainsaw (Secotom 10—STRUERS) with disc



Fig. 10 System of chemical etching



Fig. 8 PCB-FR4 substrate piece



(a)



(b)



(c)

Fig. 9 Mask of the prototypes to be realized. **a** printed on paper, **b** printed on transparent paper **c** printing on glass plates

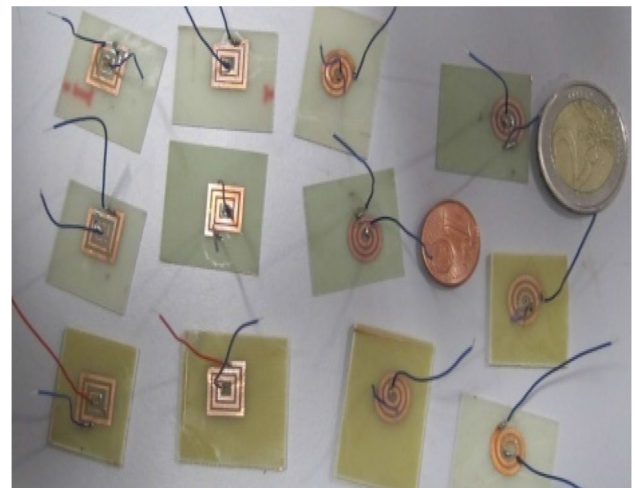


Fig. 11 Realized prototypes at LAPLACE laboratory

2.5.2 Realization of the Electric Circuit

We first realized on the flex, the copper circuits of the coils of the different topologies. Before any process, it is necessary to clean the PCB plates.

2.5.3 Preparation of the Engraving

The mask is transferred to the copper-metallized PCB-FR4 using photolithography which aims to reproduce precise patterns on different layers, whether for engraving or deposition steps, the patterns of this mask will be transferred to a movie.

Fig. 12 Measuring bench LCR meter HP(Agilent 4194A)

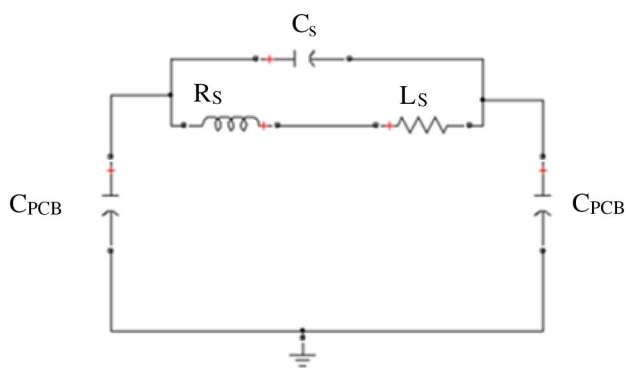
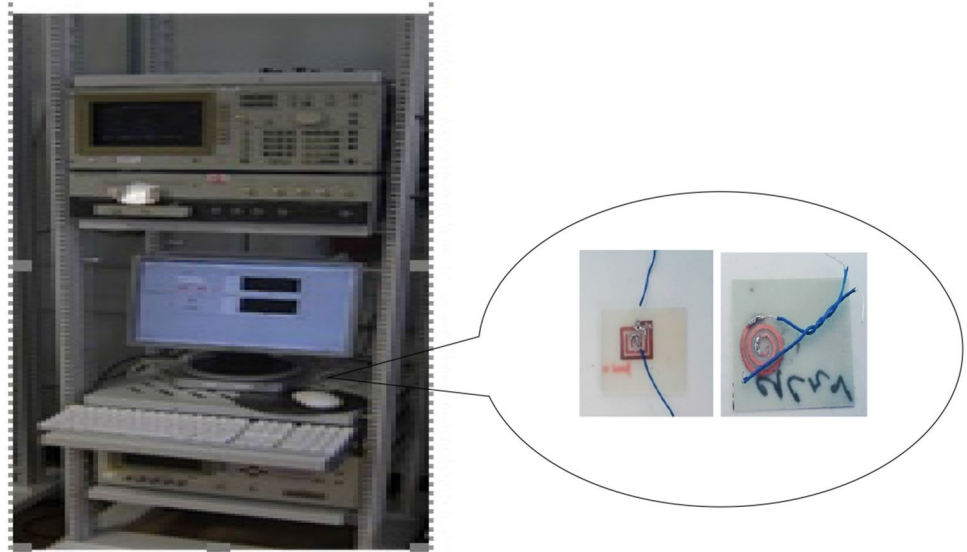


Fig. 13 Equivalent electrical circuit of a planar inductance

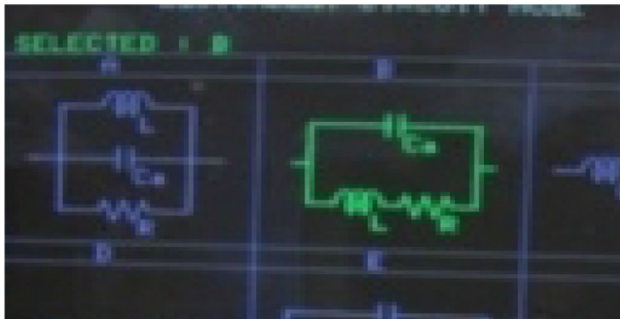


Fig. 14 Simplified circuit on the bench

2.5.4 Lamination and Photolithography of the Photosensitive Dry Film

We have printed the schematics of the different topologies of the integrated inductors on a glass plate covered with a layer of chromium in order to obtain the mask.

2.5.5 Engraving

After etching the metallized inorganic substrate and masked with iron perchloride, we removed the photosensitive film and we etched the bonding layer, that is to say eliminated copper from the surface of the flex by wet etching which allows to remove the copper on the surface of the flex. This operation consists in soaking the sample in a solution composed of iron perchloride and the water which is heated to about 27 °C. The solution preserves the copper by dissolving the part of the unprotected copper with the cured film and reveals the desired pattern.

2.5.6 Rinsing

With water of the final component in a solvent which is acetone or NaOH to remove the blue film and reveal the conductive lines.

2.5.7 Oven Passage

Pass the component in the oven at 70 °C to avoid oxidation.

2.5.8 Varnishing

The inductances realized are possibly varnished to prevent oxidation of the conductive copper.

2.5.9 The Deposit

Bonding is essential to ensure the interconnection of the central stud to the external stud.

Table 1 Geometric parameters of inductances with fixed and variable widths

Topology	All inductors		variable width	Fixed width
	l_i (cm)	t (μm)	$w1/w2/w3$ (mm)	W (mm)
Circular	4.7	35	0.3/0.6/0.9	0.9
Square	6.0	35	0.3/0.6/0.9	0.9

Table 2 Square coil with fixed width

Thickness (mm)	Rs (m Ω)	Cs (pF)	Ls (nH)	Ls/Rs (H/m Ω)
0.3	41.60	658.55	55.88	1.415
0.9	69.68	270.00	55.54	0.97
1.6	72.69	253.58	22.83	3.183

2.5.10 Realized Prototypes

Below, the realized prototypes at LAPLACE laboratory.

2.6 Characterization

The characterization of the realized prototypes requires, on the one hand, suitable measurement means and on the other hand, a model making it possible to take into account the main physical phenomena.

2.6.1 Description of the Measuring Bench

We used the measuring bench which is composed of a LCR meter HP (Agilent 4194A) which performs the vector measurement of current–voltage, and module and phase of impedance.

2.6.2 Choice of Equivalent Circuit Model

The model includes the series inductance L_s , the series resistor R_s , the coupling capacitance between the turns C_s , the capacitance associated with the substrate of PCB, the capacity of substrate.

2.6.3 Simplified physical Model of an Inductor on PCB-FR4

Figure 13 shows the equivalent scheme in π of a planar spiral coil [9, 12].

Table 3 Square coil with variable width

Thickness (mm)	Rs (m Ω)	Cs (pF)	Ls (nH)	Ls/Rs (H/m Ω)
0.3	91.82	260.01	60.22	0.65
0.9	94.19	252.58	59.47	0.58
1.6	101.6	248.52	57.71	0.22

Table 4 Circular coil with fixed width

Thickness (mm)	Rs (m Ω)	Cs (pF)	Ls (nH)	Ls/Rs (H/m Ω)
0.3	32.63	600.81	39.78	1.219
0.9	40.63	420.00	35.50	0.916
1.6	45.51	374.00	29.89	1.522

Table 5 Circular coil with variable width

Thickness (mm)	Rs (m Ω)	Cs (pF)	Ls (nH)	Ls/Rs (H/m Ω)
0.3	55.02	416.6	53.86	0.978
0.9	67.51	303.1	49.59	0.730
1.6	70.27	692.0	36.76	0.525

Table 6 Geometric parameters used for simulation

Désignations	valeurs
Number of turns n	3
Inner diameter D_{in} (mm)	1
External diameter D_{out} (mm)	1.0
Width W_F (mm)	0.9
Variable width W_v (mm)	0.3/0.6/0.9
Thickness of the conductor t (μm)	35
Perméability du PCBFR4 $\mu_{PCB-FR4}$	1
Permittivity du PCBFR4 $\epsilon_{PCB-FR4}$	4.7
Substrate thickness e (mm)	0.3/0.9/1.6

We have chosen the RLC equivalent model that supports inductance capacity and substrate resistance to measure parameters as a function of frequency [6] (Table 1).

3 Results and Discussions

3.1 Measurement Results

The tables below present the measurement results of the R_s , L_s , C_s parameters of the different planar inductances. Note from Tables 2, 3, 4 and 5 that the values of the series

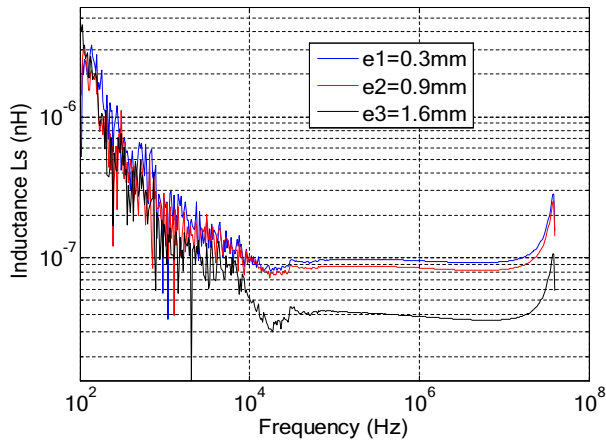


Fig. 15 Serial inductance according frequency variation case of square inductance with fixed width

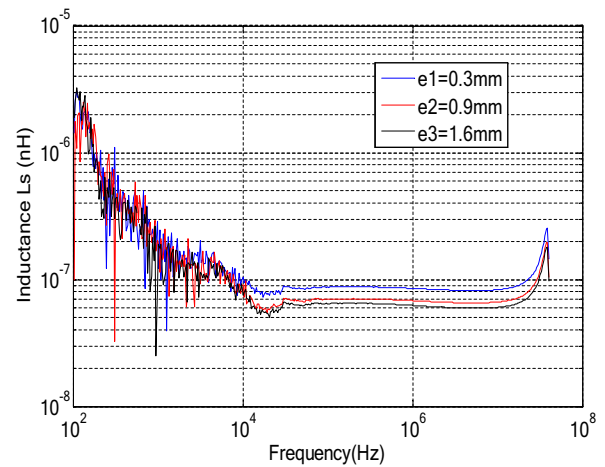


Fig. 17 Serial inductance according frequency variation case of circular inductance with fixed width

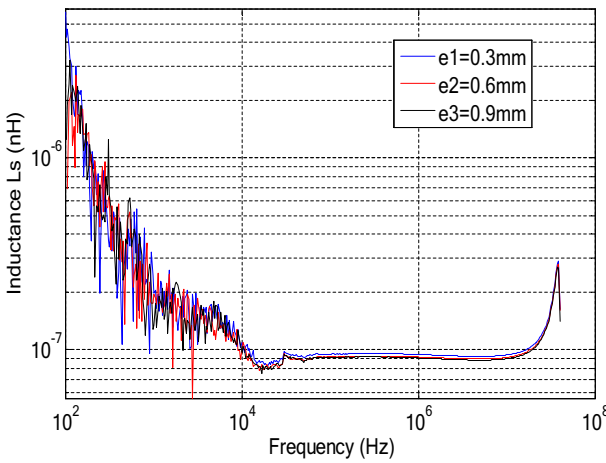


Fig. 16 Serial inductance according frequency variation case of square inductance with variable width

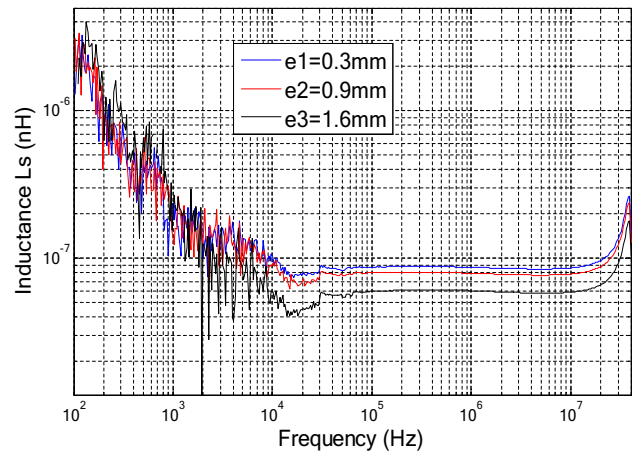


Fig. 18 Serial inductance according frequency variation case of circular inductance with variable width

resistance increase from the smallest value, which varies from 0.3 to 1.6 mm, while the series capacitance and the series inductance decrease as the thickness increases (Table 6).

3.2 Influences of Electrical Parameters on the Behavior of Micro-Coils

The results of measurements obtained with the RLC meter concern $|z|$, f and φ respectively the Z modulus, the frequency and the phase shift, for the different topologies of the micro inductances. The expressions below have allowed us to draw different curves presented in this section.

$$Z = r + jL\omega = |Z|e^{i\varphi} \quad \text{avec} \quad \omega = 2\pi f \quad (5)$$

$$|Z| = \sqrt{r^2 + (L\omega)^2} \quad (6)$$

$$R_s = \frac{|Z|}{\sqrt{1 + \tan^2 \varphi}} \quad (7)$$

$$\tan \varphi = \frac{L\omega}{r} \quad (8)$$

φ : déphasage de Z , $|Z|$: module de Z , L : Inductance

3.2.1 Inductance as a Function of Frequency

Figures 15, 16, 17 and 18 show the variation of the series inductance as a function of the frequency for all the different

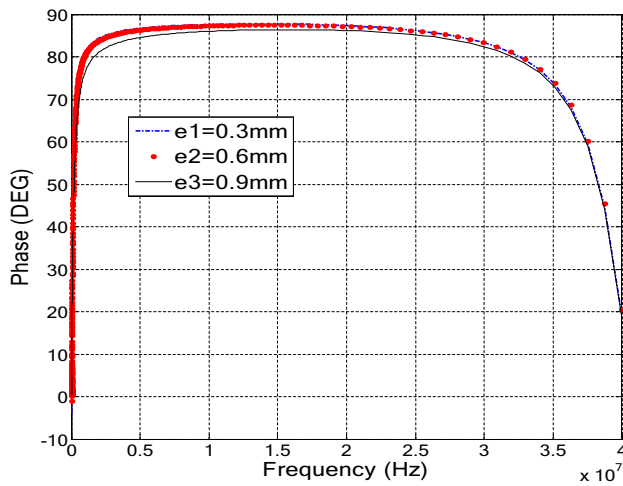


Fig. 19 Phase variation according frequency for square inductance with fixed width

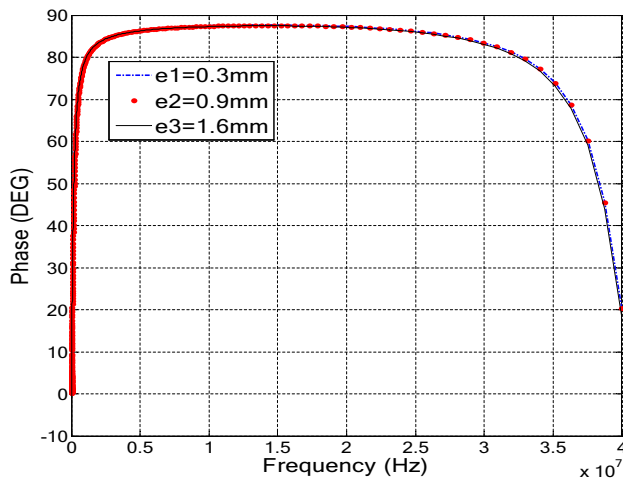


Fig. 20 Phase variation according frequency for square inductance with variable width

realize integrated coils (fixed and variable widths). The evolution of the inductance is explained by the fact that the thickness of skin in a conductor strongly depends on the frequency. The decrease of this thickness increases the ohmic resistance of the conductor and amplifies the losses by Joule effect. The increase of the resistance decreases the value of the current and consequently the value of the inductance of the micro-coils, these results are in agreement with that found in the literature [13, 14].

3.2.2 The Phase as a Function of Frequency

The Figs. 19, 20, 21 and 22 indicate the variation of the phase as a function of the frequency, in the case of a planar circular coil with a fixed and variable width, respectively.

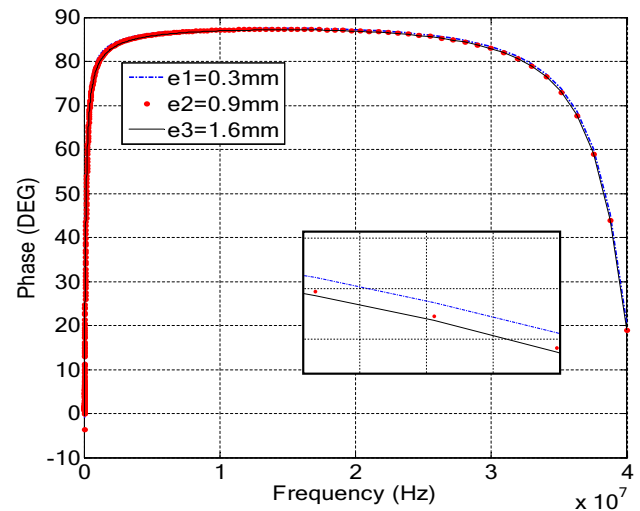


Fig. 21 Phase variation according frequency for circular inductance with fixed width

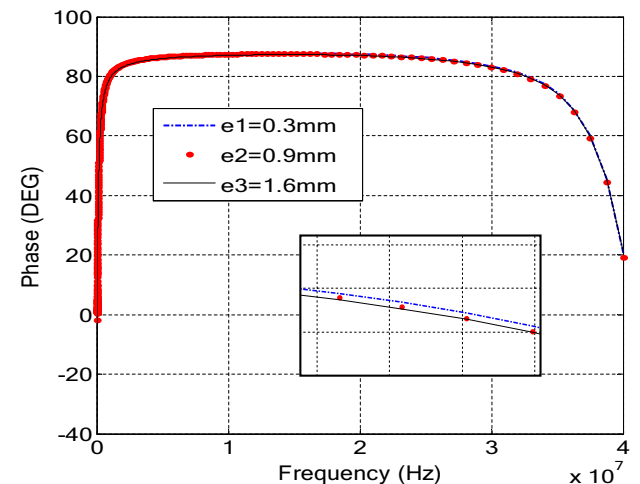


Fig. 22 Phase shift variation according frequency for circular inductance with variable width

It can be seen from these curves that the coils realizes and have a resistive and then inductive behavior. This means that the prototypes manufactured are purely inductive. This reasoning is valid for all the reels made. We also notice that the thickness influences the phase shift.

3.2.3 Resistance as a Function of Frequency

Figures 23, 24, 25 and 26 show the variation of the series resistance as a function of the frequency for the various integrated coils made (fixed and variable widths). We notice that resistance grows lo with frequency. Indeed, the increase of the frequency causes the decrease of the thickness of skin, which makes the area of the conductor where circulates the

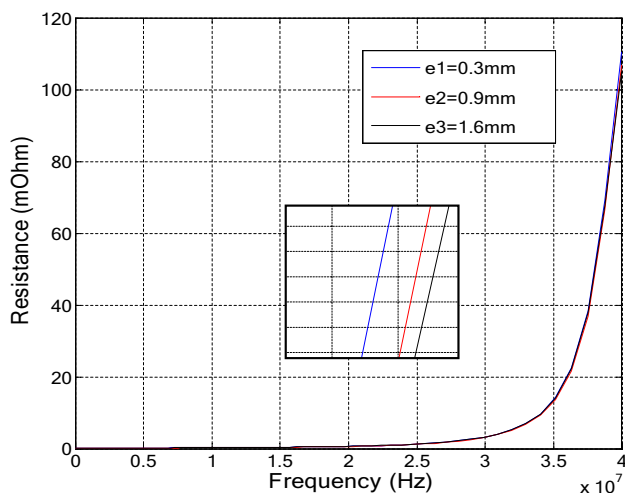


Fig. 23 Variation in series resistance depending on the frequency case of square inductance with fixed width

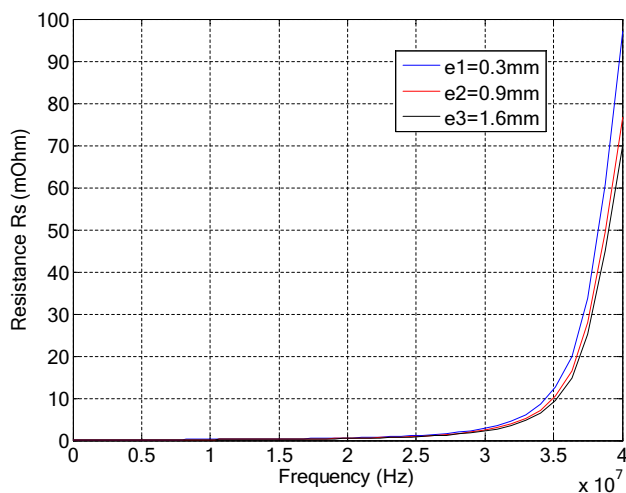


Fig. 25 Variation in series resistance depending on the frequency case of circular inductance with fixed width

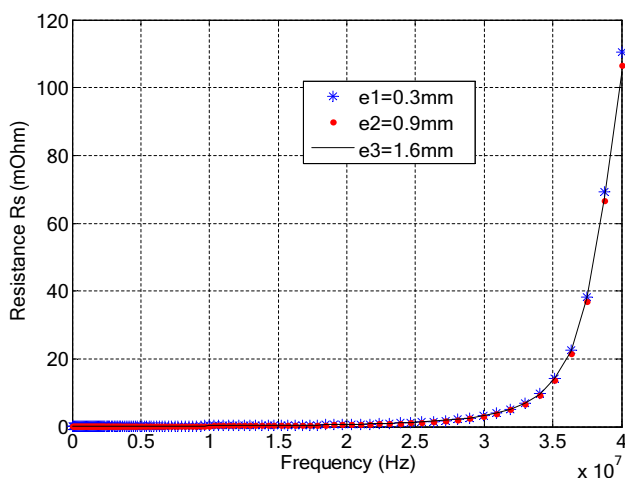


Fig. 24 Variation in series resistance depending on the frequency case of square inductance with variable width

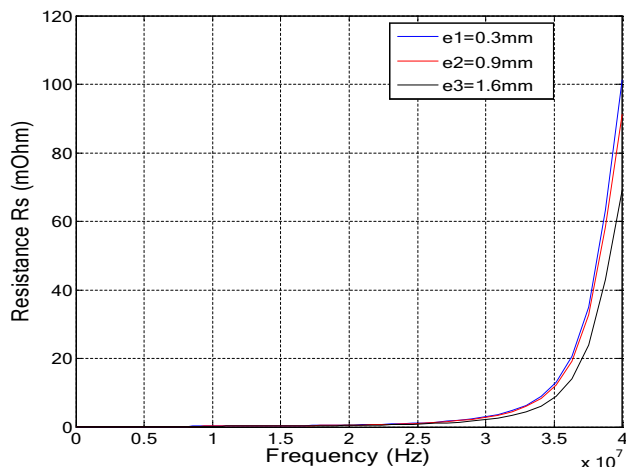


Fig. 26 Variation in series resistance depending on the frequency case of circular inductance with variable width

current of increasingly weak. The decrease of this thickness increases the ohmic resistance of the conductor and amplifies the losses by Joule effect.

Figures 27, 28 and 29 illustrate the evaluation of impedance versus frequency of standard and tapered inductors. We note that impedance is more important in the case of the tapered inductor. Higher impedance implies smaller current and hence smaller parasitic effects of the series capacitance and proximity effect. This is why a inductance with variable conductor presents, a the best behavior (Fig. 30).

3.2.4 Factor of Quality in Function of the Frequency

Figures 31, 32, 33 and 34 show the variation of quality factor versus frequency for square and circular fixed and

variable width inductors. We note that the quality factor increases until it reaches a maximum 25 value at the frequency of use of the component and then decreases beyond this value. This figure also shows that the variable width coil has the largest quality factor value for the three values of the substrate. This is because of the following reasons: the series resistance, the series capacitance, the oxide capacity and the capacitance of the substrate are less important in the case of a variable-width inductor. The variable-width coils have a higher quality factor than the standard coils which are the seat of greater parasitic effects, these results are in agreement with that found in the literature [15].

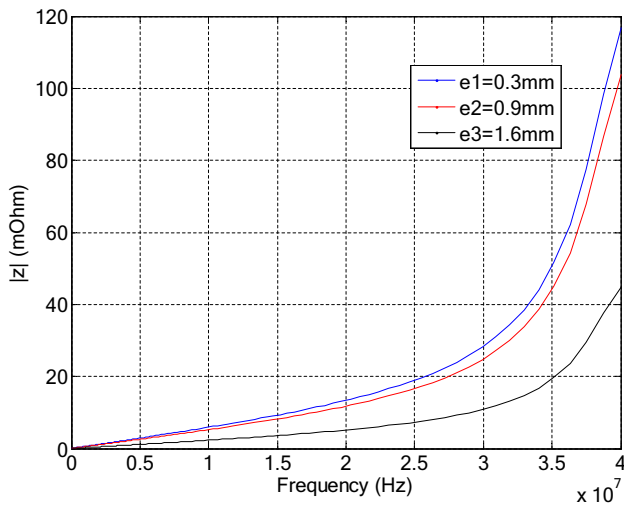


Fig. 27 Variation in the impedance depending on the frequency case of square inductance with fixed width

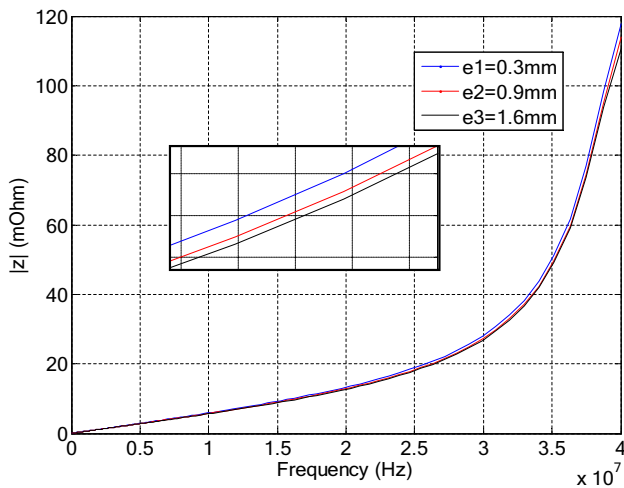


Fig. 28 Variation in the impedance depending on the frequency case of square inductance with variable width

3.2.5 Validation of our Results

Figure 35a, b respectively show the impedance and the phase shift as a function of the frequency [16]. We find that both gaits are identical to those we obtained, see Sects. 3.2.2 (Figs. 19–22) and 3.2.3 (Figs. 27–30). This comparison allows us to conclude that the sizing procedure and the implementation protocol are correct. This validates all our work (Fig. 36).

3.3 Electromagnetic Behavior of Prototypes Integrated Coils

The purpose of these simulations is to determine for both types of coils of different topologies which of those it has

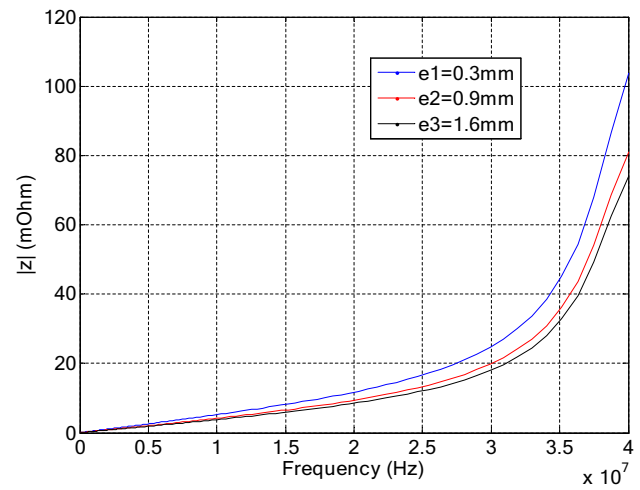


Fig. 29 Variation in the impedance depending on the frequency case of circular inductance with fixed width

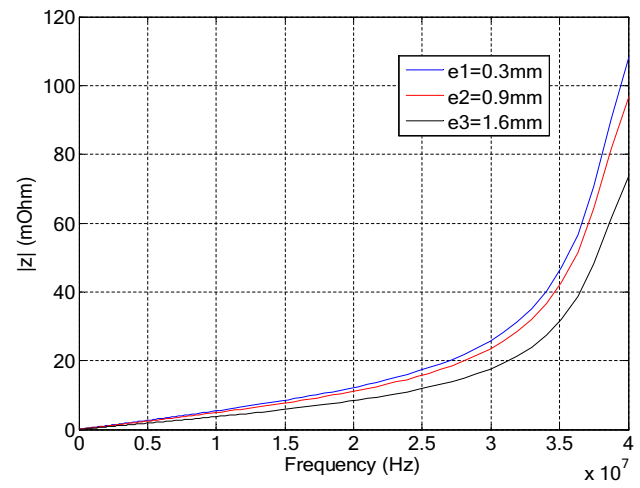


Fig. 30 Variation in the impedance depending on the frequency, case of circular inductance with variable width

an optimal distribution of current and electrical potential in the conductor and therefore it has a good distribution of the field lines. The results obtained will help us decide which topology to choose. These simulations were performed for the following frequencies: 100 Hz, $6.3246 \cdot 10^4$ Hz et $4 \cdot 10^7$ Hz.

3.3.1 Prototyping Process

Prototyping the retained coils requires several steps: Constructing the prototype geometry, defining the materials and generating the mesh. [17, 18]. material associated with each object of the geometry is identified by its physical properties. In our case, it is the copper for the turns, because we were interested mainly in the phenomena that

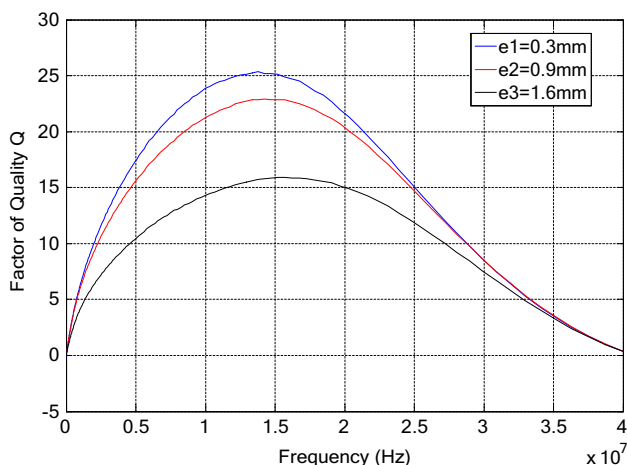


Fig. 31 Quality factor according to the frequency for fixed width square inductance

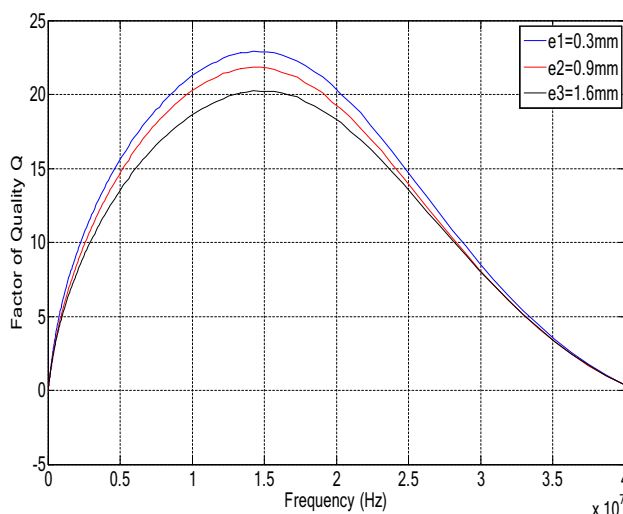


Fig. 33 Quality factor according to the frequency for fixed width circular inductance

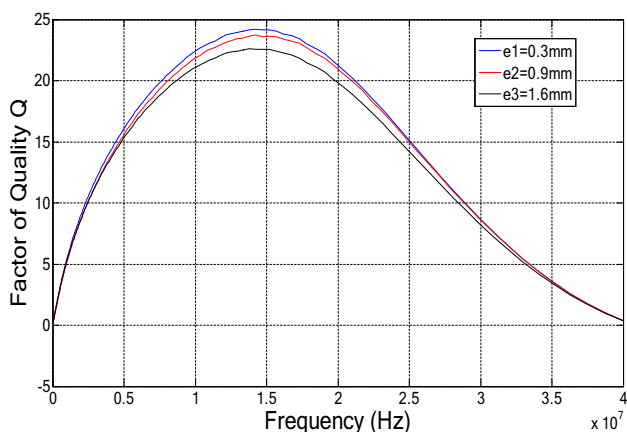


Fig. 32 Quality factor according to the frequency for variable width square inductance

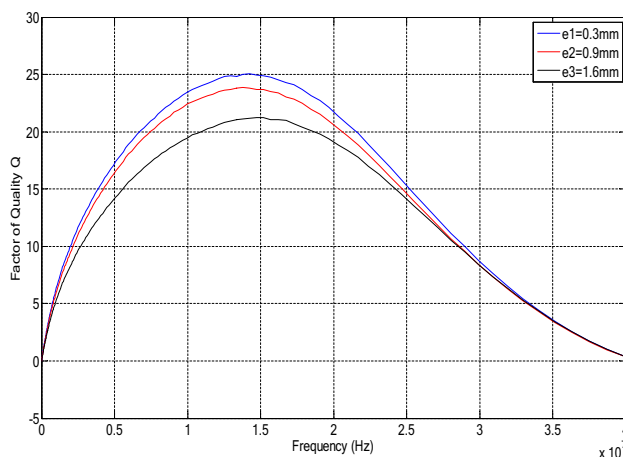


Fig. 34 Quality factor according to the frequency for variable width circular inductance

take place in the conductive ribbon with the following physical properties: $\epsilon_r = 1$, $\mu_r = 1$ and $\rho = 1.68.1020 \mu\Omega$. cm. The generation of the mesh consists of cutting the geometric model into triangles. The resolution process gives solutions to the operating frequency chosen. Figure 34a and b show the mesh of the conductors of the square and circular coils [19].

3.3.1.1 Current Density Distribution The 3D simulation results, obtained by solving the Maxwell equations by the finite element method [21], presented in this section, allow to visualize the distribution of the density of the electric current in the different topologies of coils.

- Case of fixed width coils

Figure 37a–c show the distribution of the current density in different fixed width coil topologies for $w = 0.9$ mm and for different operating frequency values. We notice that this density is minimum at the exit of the coil because of the value of the resistance of the conductor.

- Case of variable width coils

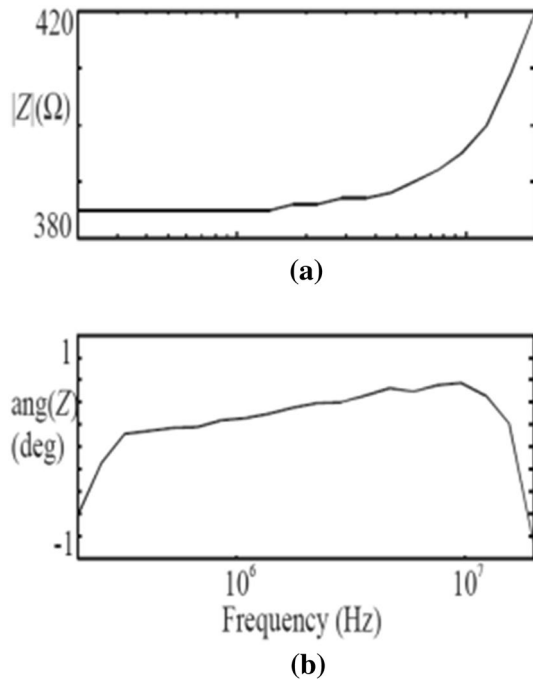


Fig. 35 Variation in **a** the impedance depending on the frequency **b** phase shift variation versus frequency [16]

Figure 38a–c show that the circular topology shows a better distribution of the current density, hence a smaller resistance. This confirms its better quality factor compared to the square topology. In deed, unlike the circular topology, the current density is not uniform in the square spirals, it is more important at the angles that induce inhomogeneous resistances in the conductors [3]. We note, that the effect of skin and proximity are present and manifest especially between adjacent turns as shown in these figures.

3.4 Examples of Applications

We realized three applications containing the prototypes of micro inductances realized. The first application, Fig. 39a is a passive audio filter. It contains a circular micro inductance fixed width and thickness of FR4 PCB $e=0.3$ mm. The second application is an active and passive/active audio filter. It contains a fixed width rectangular micro inductor with a thickness of FR4 PCB $e=0.9$ mm, see Fig. 39b. The third application is a planar-type DC buck converter DC/DC converter which contains a filter with planar inductance, see Fig. 40c.

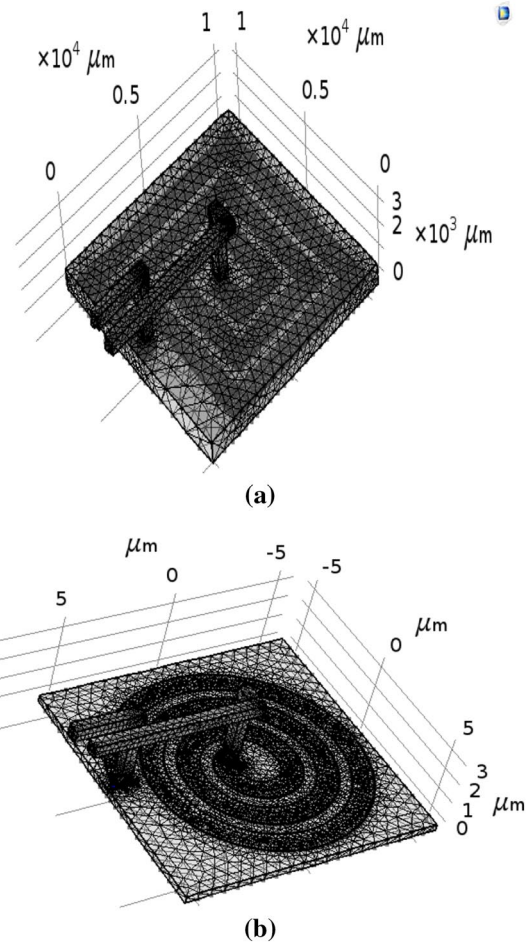


Fig. 36 Mesh of planar inductor (square and circular) [20]

3.4.1 Pictures of the Different Examples of Applications

Below, the images of the different applications.

4 Conclusion

The work presented in this paper concerns the realization of filters containing planar type inductors with fixed and variable width conductors. The geometric and electrical dimensioning of these inductors is an important step that requires taking into account many electrical and geometrical parameters. The variable width coil increases the value of the inductance. It maintains the same inductance value while reducing the proximity effect and parasitic effects of the series capacitance. The conductive spirals of all the

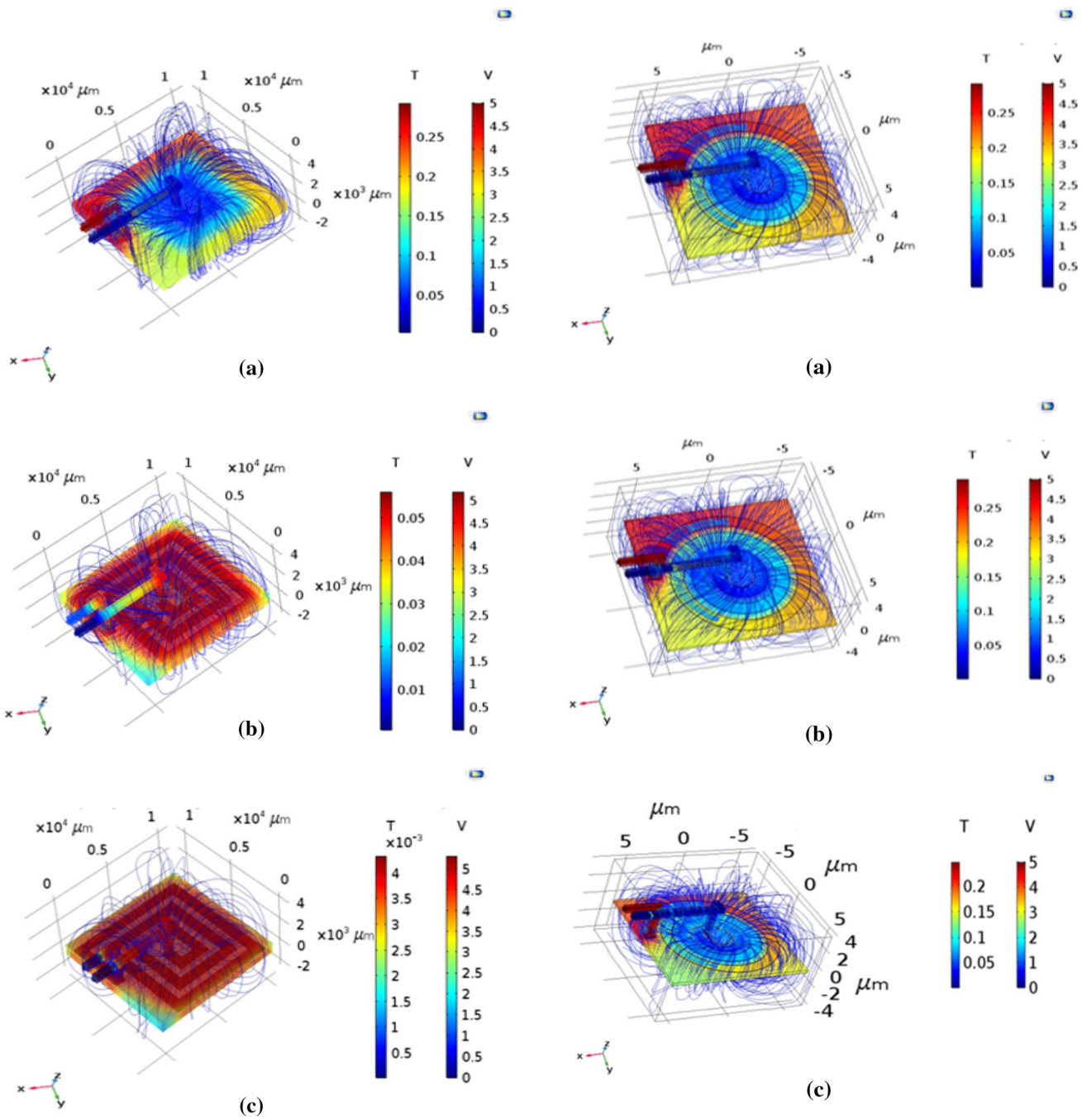


Fig. 37 Distribution of magnetic flux density and electrical potential in square standard coils for $w=0.9$ mm. **a** $f=100$ Hz, **b** $f=6.3246$ 104 Hz, **c** $f=4107$ Hz

Fig. 38 Distribution of the density of the magnetic flux and the electric potential in the circular standard coil for $w=0.9$ mm. **a** $f=100$ Hz, **b** $f=6.3246104$ Hz, **c** $f=4.107$ Hz

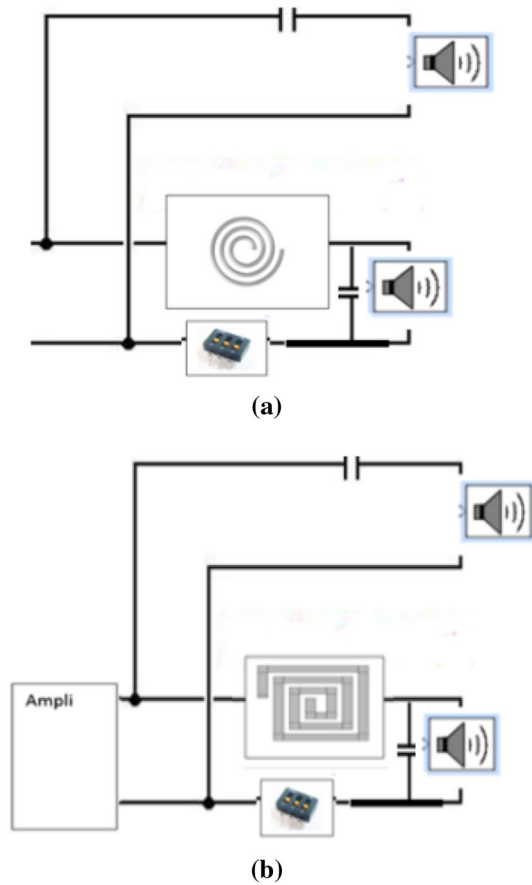
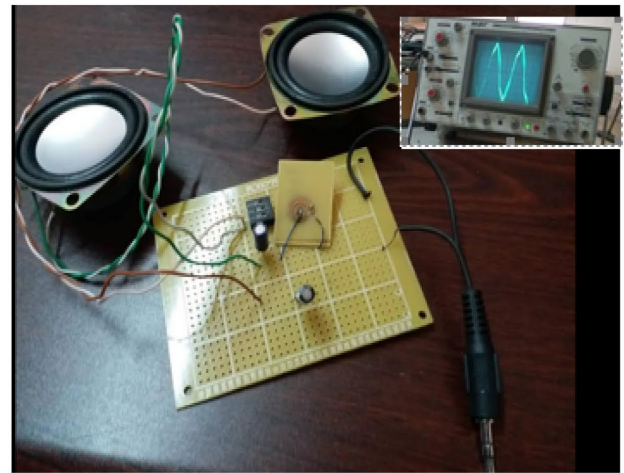
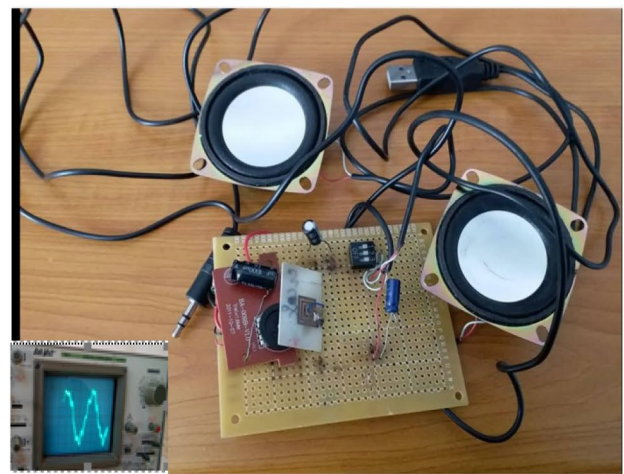


Fig. 39 Exemples of applications **a** Passif Planar Filter **b** Passif/Actif Planar Filter

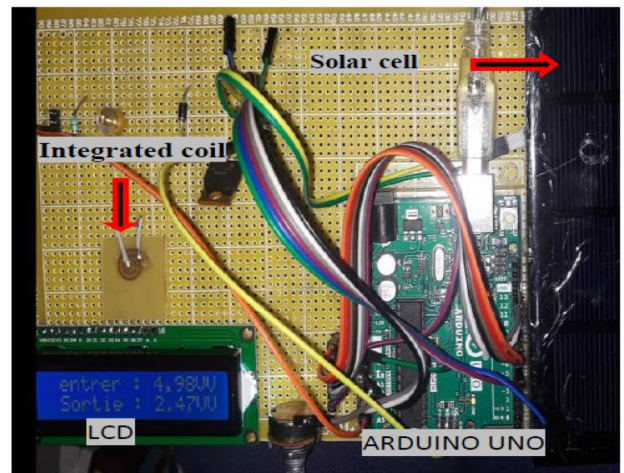
prototypes were made on the FR4 PCB whose low cost use makes it possible to respond to a very large number of applications, ranging from a few tens of kHz to several hundred MHz. The obtained results show that inductance decreases with frequency, this applies to all inductors. They also show that the two types of inductors, fixed and variable width, made on the FR4 PCB have the same electrical characteristics while occupying the same area. The maximum value of inductance is obtained with a square topology and the minimum value with a circular topology. This is due to the geometrical specifications of each topology. The electrical resistance of the square inductor is greater than that of the circular inductance for the fixed and variable width coils. Indeed, the total length of the conductor of the square inductor is greater than that of the conductor of the circular inductor. Since the impedance is greater in the case of a variable-width inductor, a low-value current flows, which implies a decrease in parasitic effects of the series capacitance and the proximity effect. The manufacture of these inductors was carried out at the Laplace laboratory in Toulouse, France.



(a)



(b)



(c)

Fig. 40 Pictures of the different examples of applications **a** second-order passive audio filter of the second order, **b** second order passive/active planar audio filter, **c** and **d** buck converter DC/DC powered by a solar cell and controlled by an arduino uno board

References

1. A.B. Islam, S.K. Islam, F.S. Tulip, *CircandSys* **4**, 237–244 (2013). <https://doi.org/10.4236/cs.2013.42032>
2. O. Bushueva, *Conception, Réalisation Et Caractérisation d'inductances et de Transformateurs Tridimensionnels Pour Applications RF et Microondes. Physique des Hautes Energies* (Université Paul Sabatier, Toulouse, 2016)
3. O. Deleagre, *Conception Réalisation et Mise en Œuvre D'un Micro-Convertisseur Intégré Pour La Conversion DC/DC* (Diss, Grenoble, 2009)
4. S. Holmstrom, A.D. Yalcinkaya, S. Isikman, C. Ataman, H.U. Koç, U. Boğaziçi FR-4 as a New MOEMS. College of Engineering, Istanbul, TURKEY and Boğaziçi. University. College of Engineering (Istanbul, TURKEY)
5. B.H. Mahamat, Y.D. Da., M.K. Youssouf, S. Capraro, J.P. Chatelon, A. Sibli, A. Désiré, J.J. Rousseau, Symposium de Génie Électrique (Cachan, France 2014). [al-01065231]
6. D.D. Yaya, *Conception, Réalisation et Caractérisation d'inductances Planaires à Couches Magnétiques* (Université Jean Monnet, Saint Etienne, 2013), p. 57
7. Laplace Laboratory on Plasma and Conversion of Energy-UMR5213, (Toulouse, France)
8. M.D. Kavimandan, *Integrated Inductors* (B.E. University of Pune, Maharashtra, 2008)
9. G. Hérault, D. Labrousse, A. Mercier, S. Lefebvre, Intégration de circuit magnétique dans le PCB dédié à un convertisseur PFC. Symposium de Génie Electrique SGE EF-EPF-MGE, GRENOBLE, France, SATIE, CNRS, ENS Cachan, Cnam, Université Paris -Saclay, (61 av. Président Wilson, 94230 Cachan, France 2016)
10. A. Désiré, *Contribution à la Réalisation d'une micro-Inductance Planaire. Thèse de Doctorat* (Université Jean Monnet, Saint Etienne, 2010), p. 177
11. C. Ravat, *Conception de Multicapteurs à Courants de Foucault et Inversion des Signaux Associés Pour le Contrôle Non Destructif* (Université Paris Sud, Paris, 2014)
12. Z. Duan, Y.X. Guo, D.L. Kwong, Rectangular Coils Optimization for Wireless Power Transmission. *Radio Sci.* **47**, RS3012 (2012). <https://doi.org/10.1029/2011RS004970>
13. B.H. Mahamat (2014) Modélisation des Inductances Planaires Intégrées, Diss, Saint Etienne
14. N.J. Oh et al., A Simple Model Parameter Extraction Methodology for an on-Chip Spiral Inductor. *ETRI J.* **28**, 1 (2006). <https://doi.org/10.4218/etrij.06.0205.0056>
15. A.S. Peng, K.M. Chen, G.W. Huang, S.C. Wang, H.Y. Chen, and C.Y. Chang, Characterization and Modeling of Silicon Tapered Inductors (1001 Ta Hsueh RD., Hsinchu 300, Taiwan, 2004)
16. S. Musunuri, P.L. Chapman, *Optimization Issues for Fully-Integrated CMOSDC-DC Converters* (University of Illinois at Urbana, 2002). <https://doi.org/10.1109/IAS.2002.1042782>
17. E. Haddad, *Conception, Réalisation, Et Caractérisation D'inductances Intégrées Hautes Fréquence* (Thèse de Doctorat soutenue à l'Université Claude Bernard, Lyon, 2012)
18. X. Margueron, *Élaboration Sans Prototypage du Circuit Équivalent de Transformateurs de Type Planar. Thèse de doctorat* (Université Joseph Fourier, Grenoble, 2006)
19. C. Wang, Determining Dielectric Constant and Loss Tangent in FR-4. UMR EMC, Laboratory Dept. of Electrical & Computer Engineering 1870 Miner Circle. MO 65409-0040. UMR EMC Laboratory Technical Report: TR00-1-041. University of Missouri (RollaRolla, 2000)
20. S.B. Shokouhian, A. Karimian, M. Zadeh, H.R.S. Rad, J. Iranian, *Med Phys* **13**(3), 193–202 (2016)
21. T.S. Johan, *IEEE Trans Power Elect.* **20**(4), 1 (2005). <https://doi.org/10.1109/TPEL.2005.850913>

Publisher's Note Springer Nature remains neutral with regard to jurisdictional claims in published maps and institutional affiliations.